

# Binder-Free $V_2O_5$ Cathode for Greener Rechargeable Aluminum Battery

Huali Wang,<sup>†</sup> Ying Bai,<sup>\*,†</sup> Shi Chen,<sup>†</sup> Xiangyi Luo,<sup>‡</sup> Chuan Wu,<sup>†</sup> Feng Wu,<sup>†</sup> Jun Lu,<sup>\*,‡</sup> and Khalil Amine<sup>\*,‡</sup>

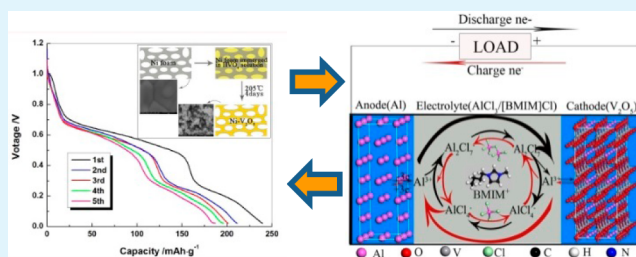
<sup>†</sup>Beijing Key Laboratory of Environmental Science and Engineering, School of Chemical Engineering and Environment, Beijing Institute of Technology, Beijing 100081, China

<sup>‡</sup>Chemical Sciences and Engineering Division, Argonne National Laboratory, 9700 South Cass Avenue, Lemont, Illinois 60439, United States

## S Supporting Information

**ABSTRACT:** This letter reports on the investigation of a binder-free cathode material to be used in rechargeable aluminum batteries. This cathode is synthesized by directly depositing  $V_2O_5$  on a Ni foam current collector. Rechargeable aluminum coin cells fabricated using the as-synthesized binder-free cathode delivered an initial discharge capacity of 239 mAh/g, which is much higher than that of batteries fabricated using a cathode composed of  $V_2O_5$  nanowires and binder. An obvious discharge voltage plateau appeared at 0.6 V in the discharge curves of the Ni- $V_2O_5$  cathode, which is slightly higher than that of the  $V_2O_5$  nanowire cathodes with common binders. This improvement is attributed to reduced electrochemical polarization.

**KEYWORDS:** aluminum battery, binder-free,  $V_2O_5$  cathode, ionic liquid electrolyte, PTFE binder, PVDF binder



The lithium-ion battery is widely used in small electronic devices, electric vehicles, and other applications. Because it has the highest energy density among the commonly used secondary batteries, the demand and proportion of the market are likely to grow. Continued effort is necessary to develop novel batteries with higher energy density, lower cost, and improved safety to meet the increased demand. Key to developing new secondary battery systems is multielectron reactions involving more than one electron transfer, which may lead to higher specific capacity and energy density.<sup>1–4</sup> Novel multielectron transfer systems under development include magnesium batteries<sup>5–7</sup> and aluminum batteries.<sup>8–14</sup>

Aluminum is the most abundant metal in the earth's crust and has a high theoretical energy density due to a three-electron transfer during the electrochemical charge/discharge reaction. As a result, battery systems containing aluminum electrodes have good promise for the future.<sup>9,15</sup> However, because the standard reduction potential of  $Al^{3+}$  is  $-1.68$  V (vs standard hydrogen electrode), reduction of the  $Al^{3+}$  in an aqueous solutions may be problematic, for it may be accompanied by a hydrogen evolution reaction.<sup>16</sup> For that reason, nonaqueous electrolytes are chosen to be used in rechargeable aluminum batteries. Room-temperature ionic liquids have been intensively investigated as electrolytes for Li-ion batteries.<sup>17–19</sup> Recently, researchers have obtained very stable electrochemical behavior in tests of rechargeable aluminum coin cells that use  $AlCl_3$  containing imidazolium-based ionic liquids as electrolyte.<sup>8,10–13</sup> This kind of ionic liquid

possesses different degrees of Lewis acidity depending on the  $AlCl_3$ : imidazolium halide ratio, and anions change with the ratio (Anions change as follows:  $Cl^- \rightarrow AlCl_4^- \rightarrow Al_2Cl_7^- \rightarrow Al_3Cl_{10}^-$  with  $AlCl_3$  mole fraction increasing)

In a previous study,<sup>8</sup> researchers found that  $V_2O_5$  can be used as the cathode material for the rechargeable aluminum battery. However, many problems remain. In most cases,  $V_2O_5$  powders are mixed with conductive additive and polymer binder to form pasted electrodes on current collectors for the electrodes preparation. As a result, the actual capacity of the electrode is lowered and the electrolyte accessibility to the active material is affected because of the presence of the inactive components, which further devalues the electrochemical performance. An alternative to the use of pasted electrodes is the direct growth of ordered nanostructures on a conducting substrate. Researchers have found that electrodes synthesized by direct growth of particles on a conducting substrate enable good electrical contact and enhanced pathways for ion transport kinetics, especially for a conductive substrate with three-dimensional network.<sup>20–23</sup> Such electrodes are conducive to the migration and diffusion of the electrolyte in the electrode, and may reduce polarization and enhance the battery voltage. In this paper, a binder-free  $V_2O_5$  cathode was synthesized by a

Received: November 18, 2014

Accepted: December 18, 2014

Published: December 18, 2014



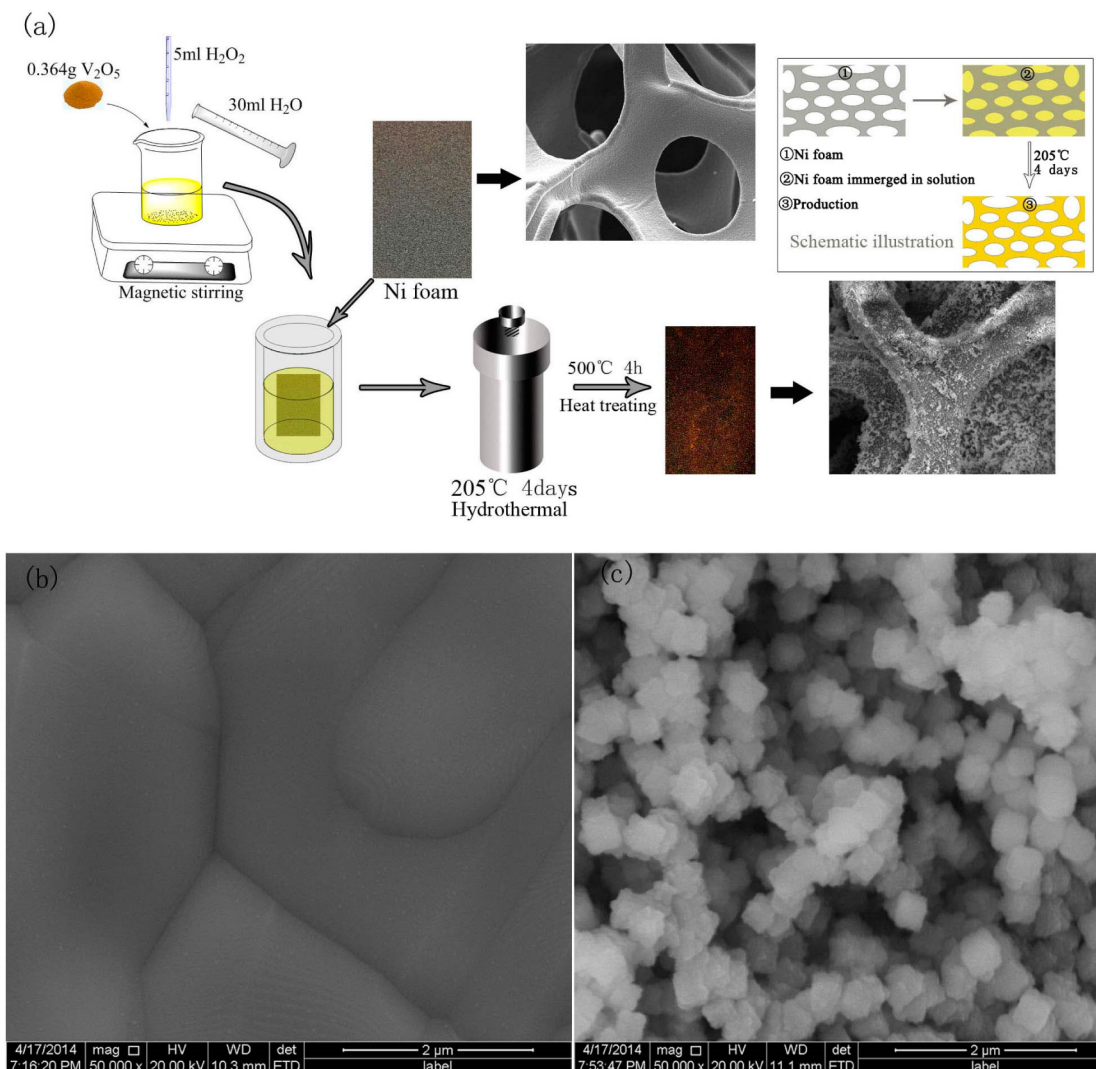


**Figure 1.** (a) Preparation process and schematic illustration for the formation of binder-free Ni–V<sub>2</sub>O<sub>5</sub>; (b) SEM image of Ni foam; and (c) SEM image of binder-free Ni–V<sub>2</sub>O<sub>5</sub>.

one-step, facile, cost-effective in situ hydrothermal deposition method. It eliminates the use of ancillary conducting material and binder, thus makes the electrode fabrication process more streamlined and greener. The cathode was tested in a rechargeable aluminum cell with acidic AlCl<sub>3</sub>/[1-butyl-3-methylimidazolium] (BMIM)Cl ionic liquids as electrolyte. The impact of binders (PVDF and PTFE) on cell performance was also assessed.

To improve the electrochemical performance of the aluminum battery and exclude the impact of possible side-reactions between the ionic liquids and the binder, a binder-free cathode material was designed and synthesized by directly depositing cathode material on a conducting substrate. A schematic diagram for the fabrication of the Ni–V<sub>2</sub>O<sub>5</sub> cathode composite is illustrated in Figure 1(a). This hydrothermal synthesis is adopted from Jayaprakash et al.,<sup>8</sup> with the difference that one piece of nickel foam substrate was added to the polytetrafluoroethylene-lined stainless steel reactor to synthesize binder-free Ni–V<sub>2</sub>O<sub>5</sub> cathode. Also, for comparison purposes, V<sub>2</sub>O<sub>5</sub> nanowire was synthesized by the Jayaprakash et al. method.<sup>8</sup>

The as-synthesized Ni–V<sub>2</sub>O<sub>5</sub> material was used as the cathode in tests with 2025 coin-type cells. These cells were

assembled in an argon-filled glovebox (MBraun Labmaster130) and had Al metal (99.9999% Al purity) as the counter and reference electrodes, AlCl<sub>3</sub>/[BMIM]Cl (mole ratio 1.1:1) ionic liquid as electrolyte, and a Whatman glass fiber (GF/C) as separator. For comparison, also tested in coin cells was a V<sub>2</sub>O<sub>5</sub> nanowire cathode with Super P carbon black and binder (mass ratio, V<sub>2</sub>O<sub>5</sub>: Super P: binder=8:1:1),<sup>8</sup> in which Ni foam was also used as the current collector. Polyvinylidene difluoride (PVDF) and polytetrafluoroethylene (PTFE) were used as binder, respectively. Galvanostatic electrochemical charge–discharge cycling of the test cells was performed on a LAND CT2001A battery test system at room temperature, under a potential window of 2.5–0.02 V, and at charge–discharge current density of 44.2 mA/g.

Schematic illustration for the formation of Ni–V<sub>2</sub>O<sub>5</sub> is shown in Figure 1a. Ni foam first immersed in pervanadic acid (HVO<sub>4</sub>) solution, and then in hydrothermal heating process, HVO<sub>4</sub> decomposed to V<sub>2</sub>O<sub>5</sub>, which deposited on the surface of Ni foam. Figure 1b, c shows magnified SEM images of the Ni foam and Ni–V<sub>2</sub>O<sub>5</sub>, respectively. From the magnified SEM image in Figure 1c, it can be seen that V<sub>2</sub>O<sub>5</sub> particles uniformly covered the Ni foam surface, and the diameter of V<sub>2</sub>O<sub>5</sub> particles is about 500 nm. These uniformly distributed particles grown

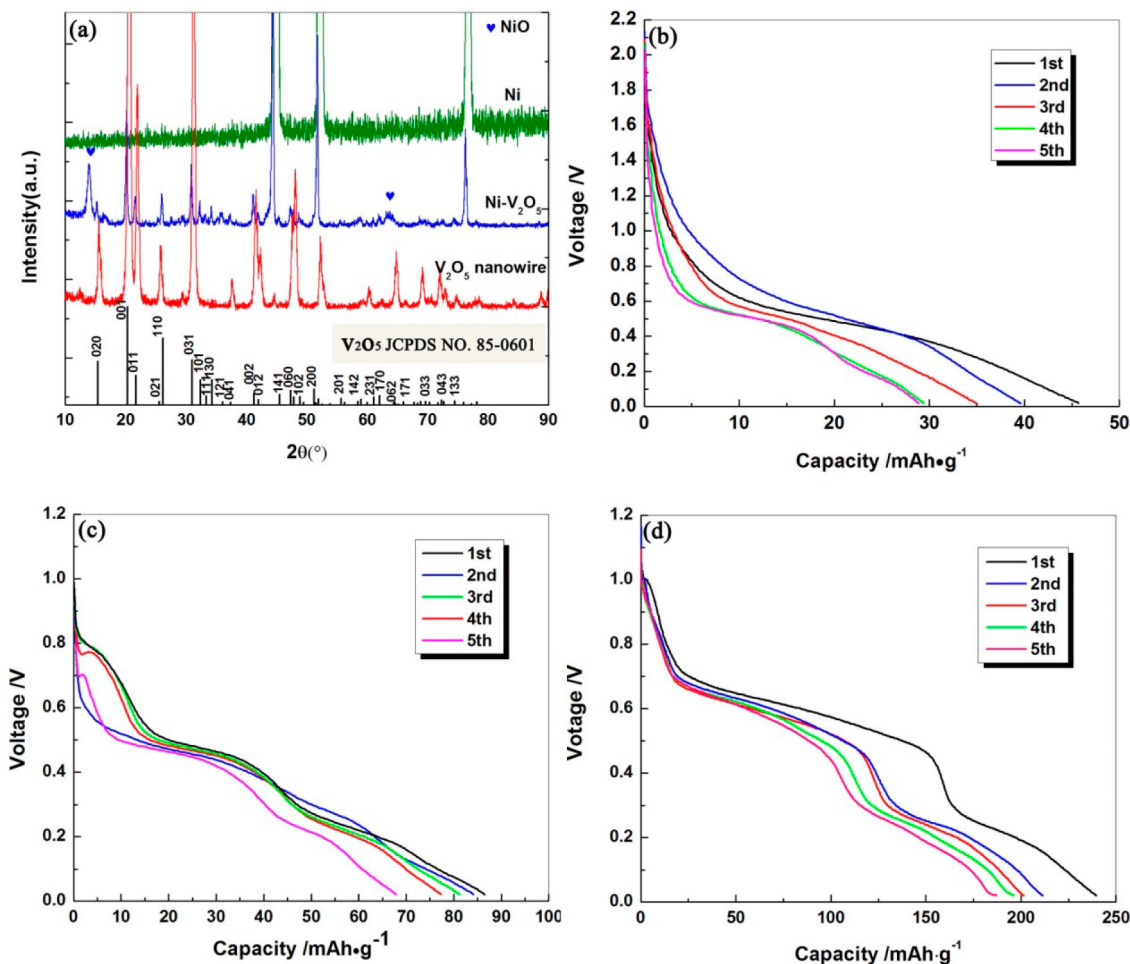


**Figure 2.** (a) XRD patterns for Ni–V<sub>2</sub>O<sub>5</sub> material, V<sub>2</sub>O<sub>5</sub> nanowires, and Ni substrate. Galvanostatic discharge profiles of cell using cathode with (b) V<sub>2</sub>O<sub>5</sub> nanowires with PVDF binder, (c) V<sub>2</sub>O<sub>5</sub> nanowires with PTFE binder, and (d) binder-free Ni–V<sub>2</sub>O<sub>5</sub>.

on a three-dimensional netlike structure conductive substrate may provide larger surface area and more ion adsorption sites, compared to V<sub>2</sub>O<sub>5</sub> nanowire cathode which active material was coated on collector, indicating that the composite material should exhibit good electrochemical performance.

XRD patterns of the prepared cathode materials are shown in Figure 2(a), along with the V<sub>2</sub>O<sub>5</sub> pattern from the JCPDS (Joint Committee on Powder Diffraction Standards) database. It can be seen that diffraction peaks for the fabricated vanadium oxides can be indexed to V<sub>2</sub>O<sub>5</sub> with *Pmmn* space group (JCPDS No. 85–0601). The patterns for the fabricated vanadium oxides show three strong peaks of the Ni substrate and some weak peaks of NiO. The NiO is generated from reaction of Ni with H<sub>2</sub>O and H<sub>2</sub>O<sub>2</sub> at elevated temperature, which first forms Ni(OH)<sub>2</sub>, and then decomposes to NiO when calcined. Since Ni is chemically stable and has compact oxide film on the surface, only a very small part of the Ni is reacted, and the amount of NiO can be overlooked.

The voltage profiles for the initial five discharges of the cells fabricated using Ni–V<sub>2</sub>O<sub>5</sub> material and V<sub>2</sub>O<sub>5</sub> nanowires as the cathode are shown in Figures 2b–d. In the voltage range of 0.02–2.5 V, the as-assembled battery using Ni–V<sub>2</sub>O<sub>5</sub> as cathode (Figure 2d) delivered an initial discharge capacity of 239 mAh/g, much higher than that of cells fabricated using V<sub>2</sub>O<sub>5</sub> nanowire as cathode (Figure 2b, c). Though these cells were charged to 2.5 V, they polarized quickly in the discharge

process, and it can be seen that the discharge voltage plateau is relatively low. An obvious discharge voltage plateau could be seen at 0.6 V in the galvanostatic discharge curves of the Ni–V<sub>2</sub>O<sub>5</sub> cathode (Figure 2d), which is slightly higher than that of the V<sub>2</sub>O<sub>5</sub> nanowire cathode. This improvement is attributed to the properties of the binder-free cathode, which not only enhanced the charge exchange between the V<sub>2</sub>O<sub>5</sub> active material and the collector Ni foam, but also improved the migration and diffusion of the electrolyte within the large-scale three-dimensional network structure of the cathode, thus reducing the electrochemical polarization.

It is noteworthy that the initial discharge capacity for the V<sub>2</sub>O<sub>5</sub> nanowire cathode using PVDF binder (46 mAh/g) is much lower than that using PTFE binder (86.5 mAh/g). This result shows that different binders can have an impact on cell performance. To explore further, we investigated the compatibility between the ionic liquid electrolyte, AlCl<sub>3</sub>/[BMIM]Cl, and the PVDF and PTFE binders.

White PVDF and PTFE powders were directly added to weighing bottles containing prepared acidic chloroaluminate ionic liquid (AlCl<sub>3</sub>/[BMIM]Cl = 1.1:1) (2 mL, 10 mg/mL) and allowed to stand for 1 h. As shown in Figure 3, the ionic liquid darkened rapidly when PVDF was added, but no reaction was evident when PTFE was added, indicating that PTFE is insoluble in the ionic liquid. These results reveal the reason for the lower discharge capacity in the cell with PVDF binder.

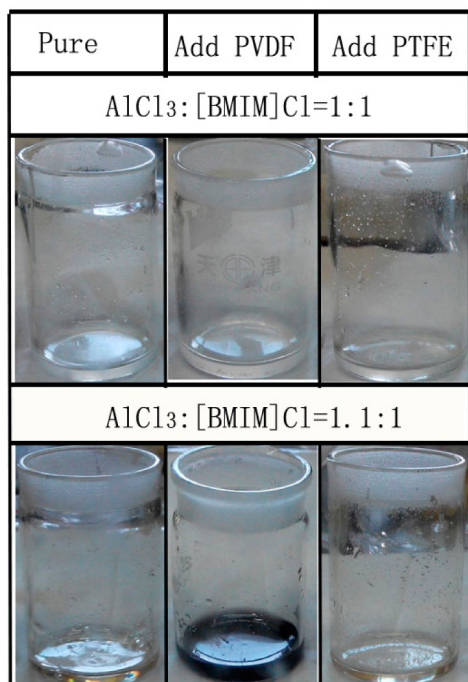
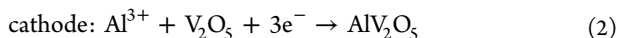
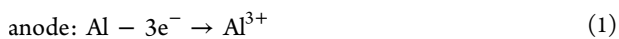


**Figure 3.** Comparison of weighing bottles with neutral (upper row) and acidic (lower row)  $\text{AlCl}_3/[\text{BMIM}]\text{Cl}$  ionic liquids to which were added PVDF and PTFE.

Because this binder is incompatible with acidic  $\text{AlCl}_3/[\text{BMIM}]\text{Cl}$  liquid, active material peeled off the cathode and lessened the discharge capacity. By contrast, neither the PVDF nor PTFE binder had any apparent reactive effect on neutral ionic liquid ( $\text{AlCl}_3/[\text{BMIM}]\text{Cl} = 1:1$ ), as also shown in Figure 3. On the basis of these results, we concluded that  $[\text{BMIM}]^+$  and  $\text{AlCl}_4^-$  have no effect on the reaction that occurred between the acidic ionic liquid and PVDF binder, but the  $\text{Al}_2\text{Cl}_7^-$  in this ionic liquid did react with the PVDF. We further inferred that PVDF binder is incompatible with all kinds of acidic chloroaluminate ionic liquids, whereas PTFE binder is more suitable for batteries that use such electrolyte.

Jayaprakash et al.<sup>8</sup> and Wang et al.<sup>11</sup> have proposed that Al ions are inserted into and extracted from vanadium oxides by a simple three-electron transfer reaction. However, Reed et al.<sup>13</sup> believe that the  $\text{V}_2\text{O}_5$  in aluminum batteries exhibits no electrochemical activity toward aluminum, and the batterylike performance can be attributed to reactions with the iron and chromium in the stainless steel current collector used in cathode. However, according to our work, aluminum batteries fabricated using Ni foam as the cathode show no electrochemical activity (Figure 4). Hence, we believe the vanadium oxides alone participate in the redox reaction.

A schematic diagram of the reaction sequence for an aluminum battery with  $\text{V}_2\text{O}_5$  cathode on discharge and charge is shown in Scheme 1. In the discharge process



In the charge process:

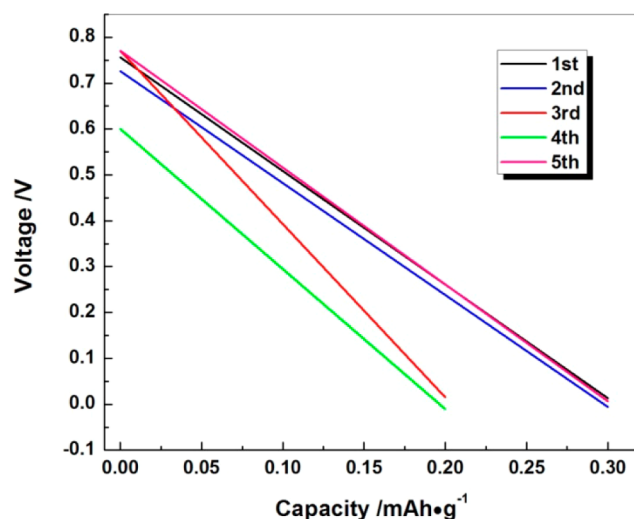
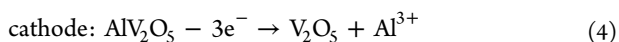
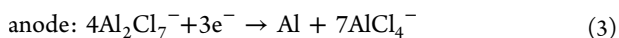
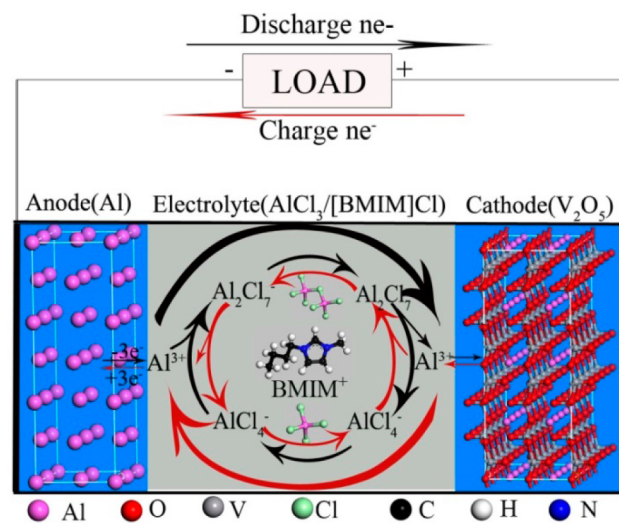


**Figure 4.** Galvanostatic discharge profiles of aluminum cell using Ni foam (calcination at 500 °C for 4 h in air) as cathode.

#### Scheme 1. Schematic Diagram of Reaction Sequence in Aluminum Battery during Charge/Discharge



However, it is mainly aluminum anions ( $\text{AlCl}_4^-$  and  $\text{Al}_2\text{Cl}_7^-$ ) that shuttle back and forth between the cathode and anode in the electrolyte in the discharge/charge process, while  $\text{Al}^{3+}$  undergoes ion exchange at the interface between the electrolyte and electrode. Because the aluminum ions in the electrolyte mostly exist in the form of anions ( $\text{AlCl}_4^-$  and  $\text{Al}_2\text{Cl}_7^-$ ), and  $\text{Al}^{3+}$  generated in formula 1 and 4 tends to form complex anions:  $\text{Al}^{3+} + 7\text{AlCl}_4^- \rightarrow 4\text{Al}_2\text{Cl}_7^-$ , only a very small amount  $\text{Al}^{3+}$  dissociate from these complex anions and exist in electrolyte. Thus, serious concentration polarization probably occurred at the electrolyte/electrode interface, leading to relatively low discharge voltage.

In an effort to improve the electrochemical performance of the aluminum battery, we investigated a binder-free cathode material, which was synthesized by in situ hydrothermal deposition of  $\text{V}_2\text{O}_5$  on Ni foam. The direct growth of  $\text{V}_2\text{O}_5$  particles on the Ni foam enabled good electrical contact and enhanced pathways for Al ion transport without the need for binder. Rechargeable aluminum coin cells fabricated using the as-synthesized Ni- $\text{V}_2\text{O}_5$  as cathode delivered an initial

discharge capacity of 239 mAh/g and a relatively high voltage plateau at 0.6 V. Both these values are improvements over cells with the common binders PVDF and PTFE. We also investigated the compatibility between the binders PVDF and PTFE and the  $\text{AlCl}_3/[\text{BMIM}]\text{Cl}$  ionic liquids used as the electrolyte. The PVDF binder was found to be incompatible with acidic chloroaluminate ionic liquids, whereas the PTFE binder was more suitable.

## ■ ASSOCIATED CONTENT

### ■ Supporting Information

Experiment details of synthesis of  $\text{Ni-V}_2\text{O}_5$  cathode material. This material is available free of charge via the Internet at <http://pubs.acs.org>.

## ■ AUTHOR INFORMATION

### Corresponding Authors

\*E-mail: [membrane@bit.edu.cn](mailto:membrane@bit.edu.cn).

\*E-mail: [junlu@anl.gov](mailto:junlu@anl.gov).

\*E-mail: [amine@anl.gov](mailto:amine@anl.gov).

### Notes

The authors declare no competing financial interest.

## ■ ACKNOWLEDGMENTS

The present work was supported by the National 973 project of China (2015CB251100), and the Program for New Century Excellent Talents in University (Grant NCET-13-0033). This work was also supported by the U.S. Department of Energy under Contract DE-AC0206CH11357 with the main support provided by the Vehicle Technologies Office, Department of Energy (DOE) Office of Energy Efficiency and Renewable Energy (EERE). The authors especially thank US-China Electric Vehicle and Battery Technology program between Argonne National Laboratory and Beijing Institute of Technology.

## ■ REFERENCES

- (1) Wu, F.; Wu, C. New Secondary Batteries and Their Key Materials Based on the Concept of Multi-Electron Reaction. *Chin. Sci. Bull.* **2014**, *59*, 3369–3376.
- (2) Braconnier, J. J.; Delmas, C.; Fouassier, C.; Hagenmuller, P. Comportement Electrochimique Des Phases  $\text{Na}_x\text{CoO}_2$ . *Mater. Res. Bull.* **1980**, *15*, 1797–1804.
- (3) Jian, Z.; Zhao, L.; Pan, H.; Hu, Y.-S.; Li, H.; Chen, W.; Chen, L. Carbon Coated  $\text{Na}_3\text{V}_2(\text{PO}_4)_3$  as Novel Insertion Electrode Materials for Sodium Ion Batteries. *Electrochem. Commun.* **2012**, *14*, 86–89.
- (4) Pan, H.; Hu, Y.-S.; Chen, L. Room-Temperature Stationary Sodium-Ion Batteries for Large-Scale Electric Energy Storage. *Energy Environ. Sci.* **2013**, *6*, 2338–2360.
- (5) Aurbach, D.; Lu, Z.; Schechter, A.; Gofer, Y.; Gizbar, H.; Turgeman, R.; Cohen, Y.; Moshkovich, M.; Levi, E. Prototype Systems for Rechargeable Magnesium Batteries. *Nature* **2000**, *407*, 724–727.
- (6) Aurbach, D.; Weissman, I.; Gofer, Y.; Levi, E. Nonaqueous Magnesium Electrochemistry and Its Application in Secondary Batteries. *Chem. Rec.* **2003**, *3*, 61–73.
- (7) Gregory, T. D.; Hoffman, R. J.; Winterton, R. C. Nonaqueous Electrochemistry of Magnesium Applications to Energy Storage. *J. Electrochem. Soc.* **1990**, *137*, 775–780.
- (8) Jayaprakash, N.; Das, S. K.; Archer, L. A. The Rechargeable Aluminum-Ion Battery. *Chem. Commun.* **2011**, *47*, 12610–12612.
- (9) Li, Q.; Bjerrum, N. J. Aluminum as Anode for Energy Storage and Conversion: A Review. *J. Power Sources* **2002**, *110*, 1–10.
- (10) Paranthaman, M. P.; Brown, G. M.; Sun, X.; Nanda, J.; Manthiram, A.; Manivannan, A. A Transformational, High Energy Density Secondary Aluminum Ion Battery In *218th ECS Meeting*; Las

Vegas, NV, Oct 10–15, 2010 ; Electrochemical Society: Pennington, NJ, 2010; p 314, 2010.

(11) Wang, W.; Jiang, B.; Xiong, W.; Sun, H.; Lin, Z.; Hu, L.; Tu, J.; Hou, J.; Zhu, H.; Jiao, S. A New Cathode Material for Super-Valent Battery Based on Aluminium Ion Intercalation and Deintercalation. *Sci. Rep.* **2013**, *3*, 3383.

(12) Rani, J. V.; Kanakaiah, V.; Dadmal, T.; Rao, M. S.; Bhavanarushi, S. Fluorinated Natural Graphite Cathode for Rechargeable Ionic Liquid Based Aluminum–Ion Battery. *J. Electrochem. Soc.* **2013**, *160*, A1781–A1784.

(13) Reed, L. D.; Menke, E. The Roles of  $\text{V}_2\text{O}_5$  and Stainless Steel in Rechargeable Al–Ion Batteries. *J. Electrochem. Soc.* **2013**, *160*, A915–A917.

(14) He, Y. J.; Peng, J. F.; Chu, W.; Li, Y. Z.; Tong, D. G. Black Mesoporous Anatase  $\text{TiO}_2$  Nanoleaves: A High Capacity and High Rate Anode for Aqueous Al-Ion Batteries. *J. Mater. Chem. A* **2014**, *2*, 1721–1731.

(15) Wang, H.; Bai, Y.; Chen, S.; Wu, F.; Wu, C. Ambient Temperature Rechargeable Aluminum Batteries and Their Key Materials. *Prog. Chem.* **2013**, *25*, 1392–1400.

(16) Liu, S.; Hu, J. J.; Yan, N. F.; Pan, G. L.; Li, G. R.; Gao, X. P. Aluminum Storage Behavior of Anatase  $\text{TiO}_2$  Nanotube Arrays in Aqueous Solution for Aluminum Ion Batteries. *Energy Environ. Sci.* **2012**, *5*, 9743–9746.

(17) Ohno, H. *Electrochemical Aspects of Ionic Liquids*. John Wiley & Sons: New York, 2005; p 38–41.

(18) Armand, M.; Endres, F.; MacFarlane, D. R.; Ohno, H.; Scrosati, B. Ionic-Liquid Materials for the Electrochemical Challenges of the Future. *Nat. Mater.* **2009**, *8*, 621–629.

(19) Han, H.-B.; Liu, K.; Feng, S.-W.; Zhou, S.-S.; Feng, W.-F.; Nie, J.; Li, H.; Huang, X.-J.; Matsumoto, H.; Armand, M.; Zhou, Z.-B. Ionic Liquid Electrolytes Based on Multi-Methoxyethyl Substituted Ammoniums and Perfluorinated Sulfonimides: Preparation, Characterization, and Properties. *Electrochim. Acta* **2010**, *55*, 7134–7144.

(20) Luo, Y.; Kong, D.; Luo, J.; Wang, Y.; Zhang, D.; Qiu, K.; Cheng, C.; Lid, C. M.; Yu, T. Seed-Assisted Synthesis of  $\text{Co}_3\text{O}_4@ \alpha\text{-Fe}_2\text{O}_3$  Core–Shell Nanoneedle Arrays for Lithium-Ion Battery Anode with High Capacity. *RSC Adv.* **2014**, *4*, 13241–13249.

(21) Takahashi, K.; Wang, Y.; Cao, G. Ni- $\text{V}_2\text{O}_5 \cdot n\text{H}_2\text{O}$  Core-Shell Nanocable Arrays for Enhanced Electrochemical Intercalation. *J. Phys. Chem. B* **2005**, *109*, 48–51.

(22) Qu, B.; Hu, L.; Li, Q.; Wang, Y.; Chen, L.; Wang, T. High-Performance Lithium-Ion Battery Anode by Direct Growth of Hierarchical  $\text{ZnCo}_2\text{O}_4$  Nanostructures on Current Collectors. *ACS Appl. Mater. Interfaces* **2014**, *6*, 731–736.

(23) Salunkhe, R. R.; Bastakoti, B. P.; Hsu, C.-T.; Suzuki, N.; Kim, J. H.; Dou, S. X.; Hu, C.-C.; Yamauchi, Y. Direct Growth of Cobalt Hydroxide Rods on Nickel Foam and Its Application for Energy Storage. *Chem.—Eur. J.* **2014**, *20*, 3084–3088.